How Adsorbate Alignment Leads to Selective Reaction

Fang Cheng,[†] Wei Ji,[‡] Lydie Leung,[†] Zhanyu Ning,[†] John C. Polanyi,[†,*] and Chen-Guang Wang[†,‡]

[†]Lash Miller Chemical Laboratories, Department of Chemistry and Institute of Optical Sciences, University of Toronto, Toronto, Ontario M5S 3H6, Canada, and [‡]Department of Physics and Beijing Key Laboratory of Optoelectronic Functional Materials & Micro-nano Devices, Renmin University of China, Beijing 100872, China

ABSTRACT There has been much interest in the effect of adsorbate alignment in a surface reaction. Here we show its significance for an electron-induced reaction occurring along preferred axes of the asymmetric Cu(110) surface, characterized by directional copper rows. By scanning tunneling microscopy (STM), we found that the heterocyclic aromatic reagent, physisorbed *meta*-iodopyridine, lay with its carbon—iodine either *along* the rows of Cu(110), "A", or *perpendicular*, "P". Electron-induced dissociative attachment with the C—I bond initially along "A" gave a chemisorbed I atom and chemisorbed *vertical* pyridyl, singly surface-bound, whereas that with C—I along "P" gave a chemisorbed I atom and a *horizontal* pyridyl, doubly bound. An impulsive two-state model, involving a short-lived antibonding state of C—I, accounted for the different product surface binding in terms of closer Cu · · · Cu atomic spacing along "A" accommodating only one binding site of the pyridyl ring recoiling from I and wider spacing along "P" accommodating simultaneously both binding sites, N—Cu and C—Cu, in the meta-position on the recoiling pyridyl ring. STM studies combined with dynamical modeling can be seen as a way to improve understanding of the role of surface alignment in determining reactive outcomes in induced reaction at asymmetric crystalline surfaces.

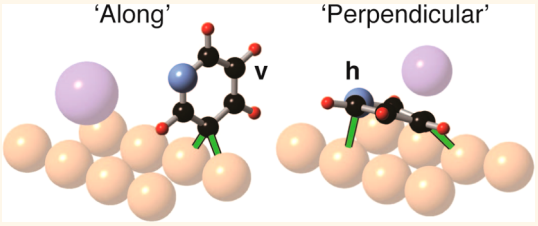

KEYWORDS: scanning tunneling microscopy · electron-induced reaction · adsorbate alignment · molecular dynamics · metal surface

Scanning tunneling microscopy (STM) of organic halides, RX, gives clear evidence of adsorbate alignment with respect to the C—X bond. Electron-induced reaction severs this C—X. Pioneering studies of the electron-induced reaction of organic halides were performed by Hla, Rieder, and co-workers,[1,2] who revealed the elementary steps underlying the Ullmann reaction for the formation of biphenyl, and by the Morgenstern group,[3] who were the first to identify electron-induced isomerization in aromatic dihalides. The interest of this laboratory has been in the molecular dynamics of the dissociative attachment event in which physisorbed organic halide gives a pair of chemisorbed reaction products,[4–6] R and X attached to a copper substrate.

The present study extends this work to a *hetero*cyclic aromatic halide, *meta*-iodopyridine, *m*-IPy. The molecular dynamics of the reaction will be shown to be affected by the presence of two atoms in the ring, C and N, that can bind strongly to the underlying metal. The reactive outcome is seen to be affected by the spacing between C and N in the reagent molecule, as compared to the spacing between the Cu atoms at the underlying surface. Solution of the equations of motion on an *ab initio* potential-energy surface shows how this complex adsorbate—substrate interaction leads to alternative reaction pathways for differently aligned reagent molecules.

Previous studies of pyridine and its derivatives on metal surfaces have clearly shown that the adsorbate binds to the surface through the N atom lone pair electrons, resulting in vertical and tilted configurations.[7–12] The physisorbed reagent *meta*-iodopyridine is shown to have two distinct molecular alignments on the asymmetric surface, Cu(110) at 4.6 K. Electron-induced reaction of each alignment is studied separately and shown unambiguously to give differently bound products at the copper surface. When the reagent was aligned with C—I approximately along the copper row of the surface in the configuration designated "A", the electron-induced reaction gave a chemisorbed I atom and chemisorbed *vertical* pyridyl bound to the surface at a single terminal carbon of the aromatic ring. By contrast, when the reagent was aligned

* Address correspondence to jpolanyi@chem.utoronto.ca.

Received for review July 8, 2014 and accepted August 7, 2014.

Published online August 07, 2014
10.1021/nn503721h

with C—I perpendicular to the Cu row, designated "P", the reaction gave a chemisorbed I atom and a *horizontal* pyridyl bound to the surface by both its carbon and its nitrogen binding sites. Solution of the equations of motion for the reaction points to the fact that substrate—atom spacing plays the major role in determining the observed differing reactive outcomes along the two major crystallographic axes of Cu(110), namely, along the rows, termed [1$\bar{1}$0], and perpendicular to them, termed [001] (these being axes "A" and "P", respectively). These selective reaction dynamics for heterocyclic halides will be shown to stem from the different spacing between the copper atoms along "A" and "P"; close-spacing (Cu···Cu = 2.55 Å) along "A" only permits one atom in the aromatic ring to bind at a time, whereas wider spacing (Cu···Cu = 4.42 Å) along "P" permits the meta-configured N and C atoms of the heterocyclic ring to bind to the surface concurrently, causing it to lie down.

The dynamics of the electron-induced reaction are well-described by an "impulsive two-state" (I2S) model introduced in earlier work,[4−6,13−15] in which the C—I bond becomes an antibond for some femtoseconds with the result that the I atom and the radical recoil in opposite directions along the prior C—I axis. In the present example, the direction of the C—I axis can be chosen by the experimenter by selecting the physisorbed *m*-IPy and placing the STM tip that delivers electrons over it to induce reaction either along "A" or "P", with markedly different outcomes. Satisfyingly, these differing outcomes are clearly evident in both experiment and theory.

RESULTS AND DISCUSSION

Two intact reagent physisorbed *meta*-iodopyridine alignments of similar heights (1.58 ± 0.04 Å) were observed by STM on Cu(110) at 4.6 K, as shown in Figure 1a,b. These two initial states exhibited markedly different reaction dynamics in electron-induced reaction, resulting in differently bound products.

The major initial state configuration (N = 452 cases) had its long axis, which we associate with the C—I bond direction, in the crystal plane at about θ = 30° to the [1$\bar{1}$0] direction. Since [1$\bar{1}$0] lies *along* the Cu rows of Cu(110), we term this physisorbed state "Along", "A". There are four equivalent "A" azimuthal directions lying at θ = ±30° to [1$\bar{1}$0] and the opposing [$\bar{1}$10] direction.

A second less abundant (N = 113 cases) physisorbed configuration was observed with its long axis at θ = ±15° to the [001] and [00$\bar{1}$] directions. Since these axes lie *perpendicular* to the Cu rows, we refer to this as "P". As in the case of the "Along" configuration, there are four equivalent perpendicular alignments.

Alignment of the carbon—halogen bonds in halobenzene molecules physisorbed on Cu(110) has previously been noted in STM studies of *p*-diiodobenzene and *p*-dichlorobenzene, performed in this laboratory. In these earlier studies of homocyclic molecules, the C—X axis of the physisorbed reagent lay with a lesser probability along [1$\bar{1}$0] but principally along the [001] axis.[4,5] Here, for a heterocyclic adsorbate, the intact physisorbed state exhibits the reverse preference, with "Along", [1$\bar{1}$0], dominating "Perpendicular", [001]. This is due to the stronger N atom binding of the aromatic ring for physisorption "Along" [1$\bar{1}$0]. We attribute the small deviations from "A" [1$\bar{1}$0] and "P" [001] alignments of *m*-IPy by 30 and 15° in the present case principally to off-axis N—Cu attraction. As noted in the introduction, evidence of attraction between the

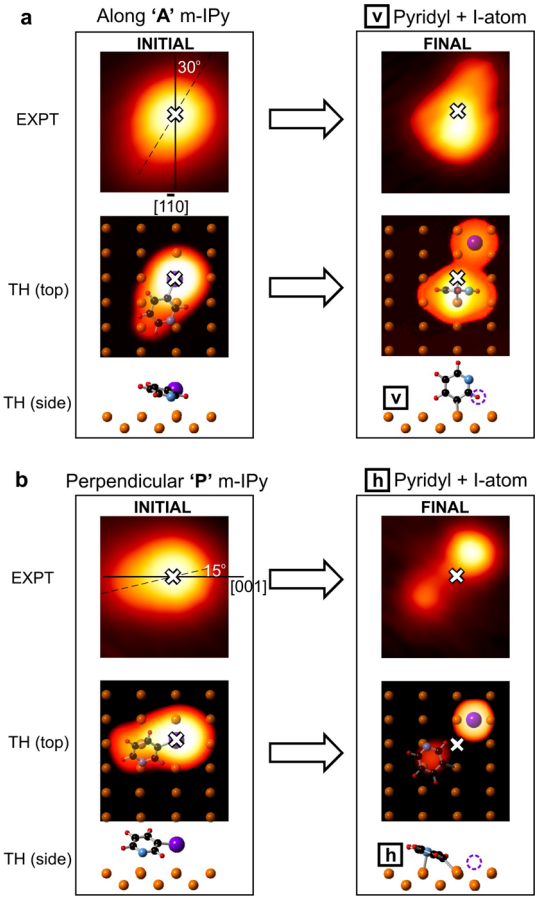

Figure 1. Electron-induced reaction of "A" and "P" *m*-IPy on Cu(110) at 4.6 K. (a) EXPT: Initial state image at left and final state (I atom and v-pyridyl) at right, obtained by STM (I = 0.5 nA and V = −0.3 V). THEORY (TH): Calculated geometries for the initial and final states are labeled as TH (top) and TH (side). The TH top view is overlaid onto its STM image simulation. The reaction products for initial state "A" were assigned by comparison with the simulated image and the measured heights for the I atom (0.60 ± 0.04 Å) and the v-pyridyl (1.12 ± 0.04 Å). (b) EXPT and TH: Initial state image at left and final state (I atom and h-pyridyl) at right. The reaction products for initial state "P" were assigned by comparison with the simulated image and the measured heights for the I atom (0.60 ± 0.04 Å) and the h-pyridyl (0.43 ± 0.04 Å). The "×" in all images indicates the reagent I atom position, which is the highest point observed in the STM images for both initial states "A" and "P". For both initial states "A" and "P", the long axis is indicated by a dashed line in the EXPT images.

N atom of pyridine and copper has been given in earlier work.[7−12]

The calculated adsorption geometries obtained by density functional theory (DFT) agreed with the experiments in leading to two physisorbed states: one broadly "Along" [1$\bar{1}$0] and one "Perpendicular" [001], corresponding to "A" and "P" in the observed STM images of the reagent, *m*-IPy. The calculations indicated that these two physisorbed configurations owed their existence to the two different ways in which a physisorbed reagent, *m*-IPy, could locate its I and N atoms simultaneously over copper atoms in the surface below. For the "A" physisorbed reagent, the underlying copper atoms lie approximately along [1$\bar{1}$0], whereas for the "P" state, they lie approximately along [001] (see the initial state pictured in Figure 1a,b, respectively). Adsorption of the physisorbed reagent can be ascribed to the polarizability of the large I atom and the bonding of the N heteroatom to an underlying copper atom. The calculated heat of adsorption is slightly greater for "A" (0.82 eV) than for "P" (0.76 eV), reflected in the fact that the "A" physisorbed molecule lies more nearly in the plane of the surface (out-of-plane tilt $\phi = 21°$) as compared with "P" (out-of-plane by $\phi = 37°$).

In this laboratory's STM studies of electron-induced reaction at copper cited above for *p*-dihalobenzenes,[4,5] the physisorption alignment was found to be the principal determinant of the recoil direction of both the halogen atom and the opposed recoil of the halophenyl organic radical. The well-defined directionality of the chemisorbed halogen atom and halophenyl products was evidence that they have not diffused following formation. This is in accordance with the fact that they remained in the same location after repeated scans. Their binding to the surface is in the region of 3 eV, explaining their immobility.

In the present work, as previously, the alignment of the physisorbed molecule governs the direction of recoil of the products. However, the presence of the attractive N atom in the aromatic ring leads to important differences in the molecular dynamics for surface reaction at copper and hence in the reactive outcomes for the different initial states "A" and "P" as compared with those observed previously.

For the present heteroaromatic reagent, the difference in alignment between the two physisorbed states, "A" and "P", can be seen from Figure 1 to have had a marked effect on the dynamics of the reaction. The final state STM images at the right in Figure 1a,b consist of two bright features in the product of the "A" reagent in contrast to the dark and bright feature in the product of "P". Computer simulations allow us to distinguish these outcomes. As is evident from the final states shown in Figure 1, the "A" reagent gave largely vertical (v) chemisorbed pyridyl (76%), whereas "P" gave almost exclusively (90%) horizontal (h) pyridyl. The height of the v-pyridyl was 1.12 ± 0.04 Å, in contrast to the h-pyridyl with a height 0.43 ± 0.04 Å. This height for the vertical chemisorbed pyridyl on Cu(110) is in approximate accord with the 1.16 Å obtained for phenyl chemisorbed after reaction of iodobenzene on Cu(110).[16] This is to be compared with the height of "in-plane", that is, horizontal, benzene measured as 0.49 Å in the Kawai laboratory.[17] The minority pathways in the present instance gave horizontal pyridyl for "A" and vertical for "P".

Computer simulation of the "v" and "h" final states of the chemisorbed pyridyl sheds light on the different bonding to the surface. For v-pyridyl, the C atom dangling bond (sp^3-hybridized) was held to a pair of Cu atoms below (binding designated C−Cu_2).[18] This "v" molecule stands up on this carbon−copper bond with a total binding computed as 2.81 eV. The N−Cu bond present in the initial state has been severed in the "v" final state due to the formation of the C−Cu bond, closely adjacent in the same copper row (Figure 1a). For h-pyridyl, by contrast, the dangling bond C atom can bind to a Cu atom at the same time as the N atom stays bound to a Cu atom in an adjacent copper row. The total calculated binding for the h-pyridyl is 2.27 eV (Figure 1b). This "h" geometry of pyridyl is, we believe, observed here for the first time.

The product angle and distance distributions for the two major pathways "A" and "P" are shown in Figure 2. The distributions for the four equivalent angles in both cases, "A" and "P", were folded to a single representative angle.

For the "A" physisorbed initial state, the C−I bond direction of *m*-IPy was found to lie 30° from the [1$\bar{1}$0] direction, as indicated in Figure 2a. The I atom and the pyridyl recoiled in opposite directions along this C−I bond direction ($N = 342$ cases). The I atoms were scattered mostly into the right trough, between Cu rows along [1$\bar{1}$0]. In one-third of the cases, the I atoms were found in the adjacent trough to the left, once again in four-fold hollow (FFH) sites. It was shown in earlier work that the I atoms diffused more readily along the troughs between Cu rows along [1$\bar{1}$0].[19] For the "A" alignment of the physisorbed *m*-IPy, the I2S model predicted that the I atom would recoil along the prior C−I axis and the pyridyl radical in the opposite direction along the same axis, both as observed in Figure 2a. The most probable distance of recoil of the I atom was observed to be 4.23 Å, and that of the v-pyridyl at 1.28 Å to the closest short bridge (S), in agreement with the distances of 4.23 and 1.28 Å obtained from the I2S model.

For the "P" initial state, the C−I bond direction of *m*-IPy was observed to be 15° from the [001] direction, as indicated in Figure 2b. The "P" physisorbed molecules produced an h-pyridyl and an I atom ($N = 102$ cases). The I atom and the pyridyl once again were found to recoil in opposite directions along the prior C−I bond. The I atom

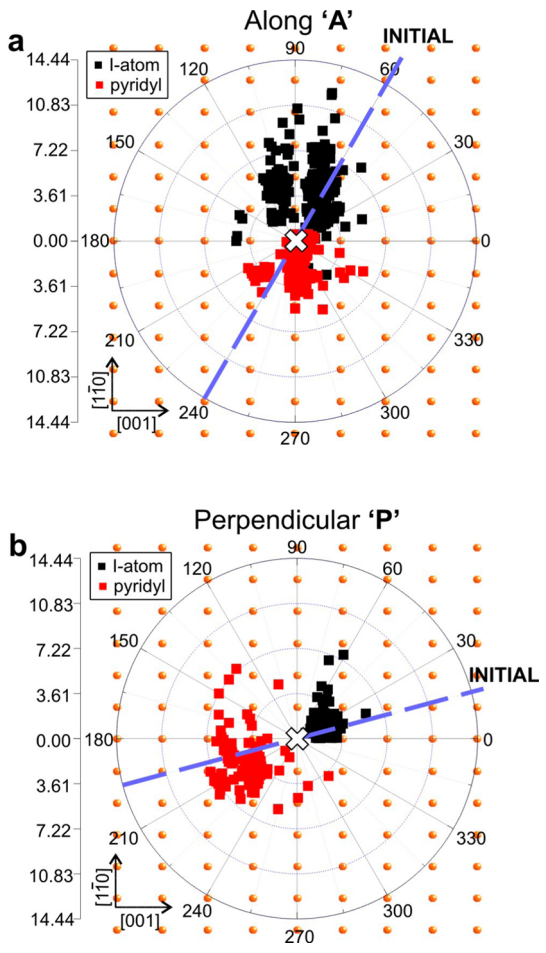

Figure 2. Product angle and distance distribution of the electron-induced reaction for "A" and "P" *m*-IPy. (a) Distribution of I atoms (red) and pyridyls (black) after electron-induced reaction of *m*-iodopyridine for the "A" alignment (*N* = 342). (b) Similarly, the product distributions for the "P" *m*-IPy (*N* = 102). The "×" gives the location of I atom in the reagent. The initial states, "A" and "P", are observed at four equivalent angles, but the data have been folded to one representative angle. The dashed lines give the direction of the principle axis of the *m*-IPy in the initial states for "A" and "P". The underlying Cu substrate is indicated.

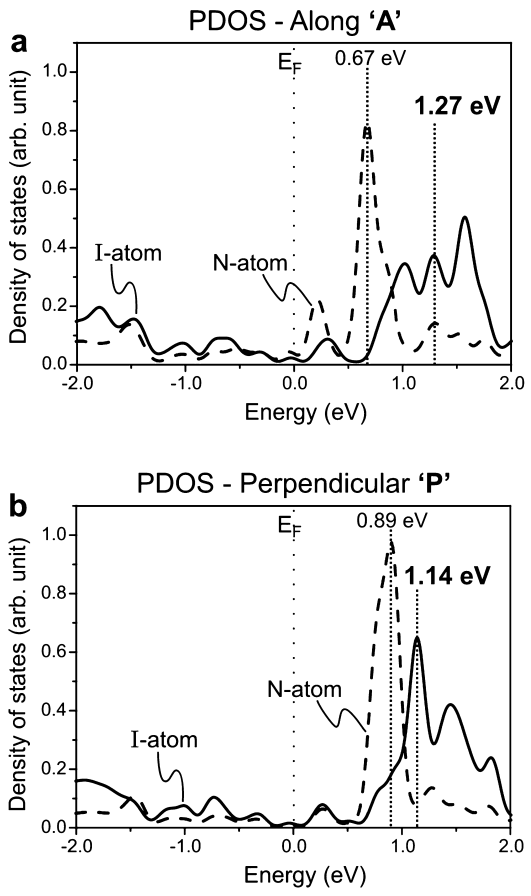

Figure 3. Projected density of states for "A" and "P" alignments. (a) PDOS of physisorbed "A" *m*-IPy on Cu(110). The LUMO is found at 0.67 eV and the LUMO+1 at 1.27 eV. (b) PDOS of physisorbed "P" *m*-IPy on Cu(110). The energies of the LUMO and LUMO+1 are located at 0.89 and 1.14 eV. The projections onto the I atom and the N atom are given by solid and dashed lines.

was observed to travel only 2.21 Å to the nearest FFH and the pyridyl by 4.42 Å to the second on-top copper site. The I2S theory predicted a qualitatively similar behavior, 3.12 Å recoil for I and 3.48 Å for pyridyl. (The observed product distributions for I atoms and pyridyls are shown in Supporting Information Figure S1 for both pathways "A" and "P".)

Figure 3 shows the projected density of states (PDOS) of physisorbed *m*-IPy in its "A" and "P" molecular alignments for the I atom and the N atom. The PDOS of the C atom bound to the I atom has the same features as the ones calculated for the I atom, in both alignments. The projected electron density located at 0.67 and 0.89 eV for the "A" and "P" initial states correspond to the π^* orbitals of the lowest unoccupied molecular orbital (LUMO). By contrast, the projected electron density corresponding to the LUMO+1 at 1.27 and 1.14 eV, for "A" and "P", exhibits additional density placed on the C−I antibonding orbital, corresponding to the σ^* orbitals. The electron density for the "P" molecular alignment at 0.89 and 1.14 eV is shown in Supporting Information Figure S2. A comparison of the LUMO+1 and the threshold for "A" and "P" electron-induced reactions (∼1.40 eV) showed that the electron entered the LUMO+1 C−I antibonding orbital in both molecular alignments. At threshold, the measured electron yields were approximately 2 and 4 × 10^{-11} for reagents "A" and "P", respectively. For the "A" initial state LUMO+1 (σ^* orbital), the ratio of charge density between the N and I atoms is 0.4:1. In contrast, the contribution of the N atom to the LUMO+1 of the "P" initial state was negligible. These findings were used as a guide for distributing the added charge between the I and N atom for the "A" initial state.

The I2S model clearly differentiated the dynamics for reaction along "A" and "P", as shown in Figure 4, which depicts the results of the *ab initio* molecular dynamics. The model for some femtoseconds (see below) replaced the C−I bond in the reagent with an antibond, due to the added unit charge. For case "A" (Figure 4a),

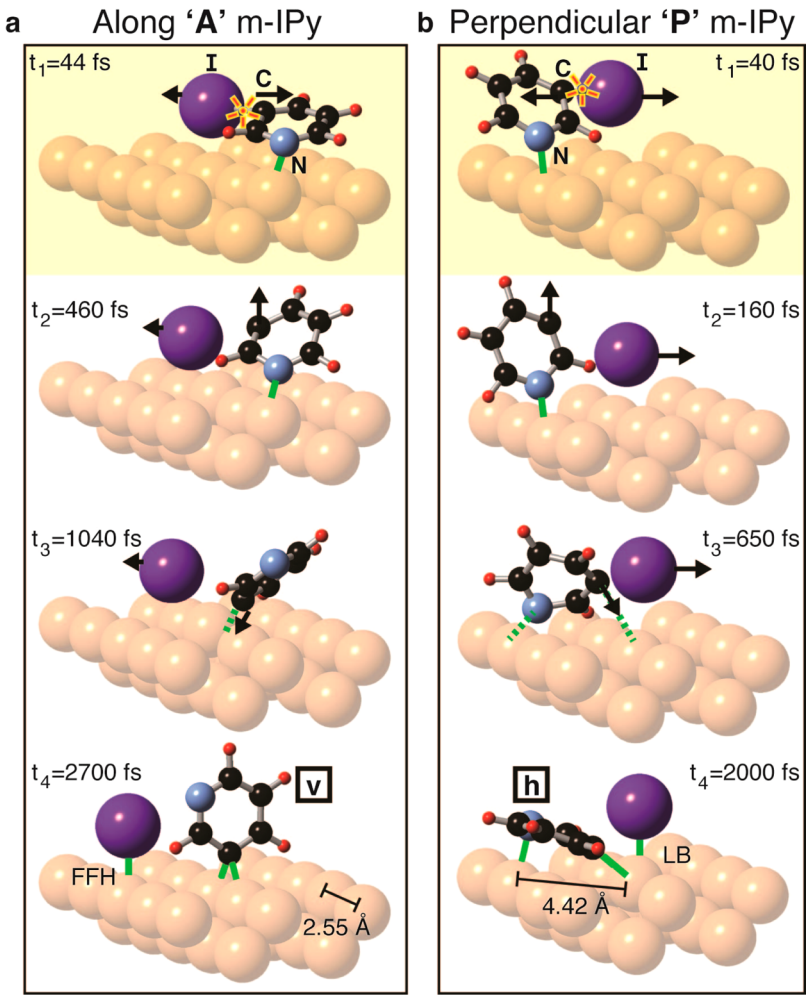

Figure 4. Molecular dynamics for the *m*-IPy reaction at the Cu surface from the I2S model. (a) "A" reaction: After 44 fs on the anionic state, yellow background, the *m*-IPy returned to the ground state, and the repulsion (arrows) caused the C−I bond to break, while pyridyl remained bound to the surface by its N atom (green line). At 460 fs, the I atom recoiled along "A" and the C atom upward (arrow). At 1040 fs, the strong carbon-to-copper attraction (green dashed line) caused C to replace N at the surface. At 2700 fs, the I atom was bound at a FFH site, and the pyridyl vertically bound. (b) "P" reaction: After 40 fs on the anionic state, yellow background, *m*-IPy returned to ground state, and the repulsion (arrows) caused the C−I bond to break, while pyridyl remained bound to the surface by its N atom (green line). At 160 fs, the I atom recoiled along "P" and the C atom upward (arrow). By 650 fs, an extended C−Cu bond formed (green dashed line), with lateral displacement of the bound N atom. At 2000 fs, the I atom was at the long bridge (LB) site, and the pyridyl bound horizontally by both N−Cu and C−Cu bonds. The Cu−Cu distance within a row and across two adjacent rows is shown in the figure.

the added negative charge was, as in previous studies, placed largely on the I atom (0.8 e^-). Here, the small residual charge was located at N ($0.2e^-$). A minimum residence time (t^*) of 44 fs was required on the anionic potential to give subsequent reaction across the ground state. At t = 460 fs on the ground state, the I atom had recoiled along "A" and the adjacent C atom of the aromatic ring had moved away from the surface, due to release of strain in the pyridyl ring. Significantly, by 1040 fs, attraction of the dangling bond C atom was moving it toward the surface to form a carbon−copper bond that replaced the nearby N−Cu bond located in the same copper row. By 2700 fs, the pyridyl was vertical, held by a strong bond C−Cu_2 bond. The final vertical state resembled phenyl on copper, computed by Lorente and co-workers.[18] As a check, we repeated our calculations of "A" with the additional electron placed exclusively on the I atom and alternatively with the added charge equally divided between the I and the N. Path "A" nonetheless invariably led to vertically bound pyridyl. For the case of "P", we only considered the case where the added charge was fully on the I atom because the contribution from the N atom to LUMO+1 (see Figure 3b) was negligible.

The molecular dynamics for path "P" are shown in outline in Figure 4b. As before, in "A", by t^* = 40 fs, the I atom and the released dangling bond C atom of the aromatic ring recoiled from one another along the prior C−I axis. At 160 fs, the I atom had moved along "P", while the released dangling bond C atom moved upward, as the recoiling ring lifted 70° out-of-plane. By 650 fs, the dangling bond C atom was approaching its binding site at the surface. This resulted in a distortion of ~17° of the pyridyl ring, while the N atom

interacted with the Cu substrate. In contrast to pathway "A", the N—Cu bond, which was located on an adjacent copper row, existed throughout. The site of this N—Cu bond shifted, however, in the course of the reaction by one copper atom along its row. As a result of this double bonding by both C and N, the final state, at 2000 fs, comprised horizontal pyridyl. The distance between the bonding sites of the C and N atoms along "P" was 4.37 Å, which matched the inter-row separation. This separation is in marked contrast to the Cu···Cu separation within a row, along "A", which is only 2.55 Å, too short to accommodate an adjacent C and a N atom bond which preferentially bind ~4 Å apart. This large spread between the C and the N binding sites, as is evident in the visualization at the bottom of Figure 4b where the separation is shown as 4.42 Å, is due in part to the fact that the C and the N are separated in a meta-location on the ring and in equal part to the fact that the sp^3 hybridization of the C dangling bond (at the right) is directed away from the ring.

CONCLUSIONS

We have extended our previous STM studies of the electron-induced reaction of homocyclic aromatic halides at Cu(110) to the case of a heterocyclic molecule, *meta*-iodopyridine, *m*-IPy. As in our previous work, the initial physisorbed molecule at 5 K when subjected to low-energy electrons coming from the STM tip formed chemisorbed products. In the present case, the products were chemisorbed atomic I plus pyridyl. The reaction dynamics can be understood once again in terms of the I2S model introduced earlier, in which the equations of motion are solved on the repulsive anionic state (duration $t^* \sim 40$ fs) and subsequently on the ground potential-energy surface. This model, based on interactions computed *ab initio*, explains the observed recoil of the I atom in one direction and that of the pyridyl in the opposite direction.

In the present work, two alignments were found for the physisorbed reagent, *m*-IPy, both experimentally by STM and also by DFT-based calculations. These two alignments were along the copper rows, denoted "A", or perpendicular to the rows, "P". By placing the tip over an adsorbate molecule aligned along "A" or "P", reaction could be initiated along a selected surface axis. Persistence of alignment in going from reagents to products was observed, as in our previous studies. Hence, by selecting "A" or "P" adsorbate, we determined the preferred axis of reaction as the fragments recoiled across the surface.

The novelty here is the observation of different reaction paths for the orthogonal crystal axes, "A" and "P". The difference in dynamics along these two directions was readily observed by STM as being the formation of vertical chemisorbed pyridyl for reaction induced along "A", in contrast to the formation of horizontally bound pyridyl for reaction along "P". Different reaction dynamics along crystal axes "A" and "P", corresponding to that found experimentally, were also clearly evident in the I2S model.

Examination of these alternative reaction pathways along the different crystal axes showed the cause of the product selectivity to be the difference in spacing between the copper atoms along "A" (2.55 Å) as compared with "P" (4.42 Å). The separation between the C—Cu and N—Cu bonds was restricted by their attachment to pyridyl. In case "A", the Cu···Cu separation at the surface accommodated only one of these bonding atoms, C or N, at a time, so that the pyridyl came to rest held *vertically* by its strong carbon—copper attachment at the position of its dangling bond. Crucial to the selective dynamics was the fact that the larger Cu···Cu separation along "P", in contrast to "A", permitted simultaneous formation of C—Cu with an sp^3-hybridized carbon dangling bond and also a N—Cu bond held at the meta-position to this on the aromatic ring. The two-fold binding of the pyridyl to the surface along "P" was responsible for holding the pyridyl, when formed along that axis, in the *horizontal* configuration.

METHODS

The experiments were conducted in a low-temperature ultrahigh vacuum STM (Omicron) system with base pressure of $<3.0 \times 10^{-11}$ mbar. The Cu(110) single crystal was cleaned by repeated cycles of Ar^+ sputtering (0.6 keV, 7 μA) followed by annealing at 800 K, until no contamination could be detected by STM. Commercially available *m*-iodopyridine, *m*-IPy (Sigma-Aldrich, 98%), was purified by multiple freeze—pump—thaw cycles and then dosed from a capillary tube directed at the Cu(110) surface. The copper crystal reached a maximum temperature of 8.6 K during dosing. The sample was then cooled, and the STM images were taken at 4.6 K. Dissociation of *m*-IPy was electron-induced by placing the STM tip over the middle of the *m*-IPy feature and maintaining a constant bias voltage of 1.40 V, with the feedback loop disabled for up to 1 s. Here, the bias voltage refers to the sample. The product positions with respect to the position of the physisorbed reagent were measured using WSxM.[20]

Theoretical simulations, including the ground state of the physisorbed *m*-IPy, the products of the electron-induced reaction, the molecular dynamics trajectories, the electronic structures, and the STM image simulations were carried out using the general gradient approximation for the exchange-correlation potential,[21] the projector-augmented wave method,[22,23] and a plane wave basis set as implemented in the Vienna ab initio simulation package.[24,25] Revised Perdew—Burke—Ernzerhof,[26] with the second version of Grimme's dispersion corrections,[27] was employed in structural relaxation, adsorption energy, and molecular dynamics calculations. This van der Waals correction was applied at ~4000 successive steps in the reaction dynamics calculation. The energy cutoff for the plane wave basis was set to 400 eV for all configurations. A supercell (5×7) consisting of 175 copper atoms in 5 layers, with at least 15 Å vacuum region, was employed to model the Cu surface. The surface Brillouin zones of the system were sampled using the gamma point only. In geometry optimizations, all atoms except those for the

bottom two Cu layers were fully relaxed until the residual force per atom was less than 0.02 eV/Å. The I2S model,[4−6,13−15] described elsewhere in detail, incorporates an anionic state of duration t^* simulated by a pseudopotential approach.[23,28,29] The molecular dynamics in the anionic state were calculated until t^*. The system was then returned to the ground state with atomic momenta and positions taken from the excited state. The dynamics were then continued until the final state was achieved.

Conflict of Interest: The authors declare no competing financial interest.

Acknowledgment. This work was funded by the Natural Sciences and Engineering Research Council of Canada (NSERC) and Xerox Research Centre Canada (XRCC). Computations were performed on TCS at SciNet HPC Consortium funded by the Canada Foundation for Innovation. SciNet is funded by the Canada Foundation for Innovation under the auspices of Compute Canada; the Government of Ontario; Ontario Research Fund−Research Excellence; and the University of Toronto.

Supporting Information Available: Figure showing the distribution of the products from the electron-induced reaction of the "A" and "P" initial states, and a comparison between the LUMO and LUMO+1 of the "P" physisorbed initial state. Two movies for the molecular dynamics of the "A" and "P" reaction. This material is available free of charge *via* the Internet at http://pubs.acs.org.

REFERENCES AND NOTES

1. Hla, S.-W.; Bartels, L.; Meyer, G.; Rieder, K.-H. Inducing all Steps of a Chemical Reaction with the Scanning Tunneling Microscope Tip: Towards Single Molecule Engineering. *Phys. Rev. Lett.* **2000**, *85*, 2777–2780.
2. Hla, S.-W.; Meyer, G.; Rieder, K.-H. Inducing Single-Molecule Chemical Reactions with a UHV-STM: A New Dimension for Nano-science and Technology. *ChemPhysChem* **2001**, *2*, 361–366.
3. Morgenstern, K. Isomerization Reactions on Single Adsorbed Molecules. *Acc. Chem. Res.* **2009**, *42*, 213–223.
4. Leung, L.; Lim, T.; Ning, Z.; Polanyi, J. C. Localized Reaction at a Smooth Metal Surface: *p*-Diiodobenzene at Cu(110). *J. Am. Chem. Soc.* **2012**, *134*, 9320–9326.
5. Eisenstein, A.; Leung, L.; Lim, T.; Ning, Z.; Polanyi, J. C. Reaction Dynamics at a Metal Surface; Halogenation of Cu(110). *Faraday Discuss.* **2012**, *157*, 337–353.
6. Huang, K.; Leung, L.; Lim, T.; Ning, Z.; Polanyi, J. C. Single-Electron Induces Double-Reaction by Charge Delocalization. *J. Am. Chem. Soc.* **2013**, *135*, 6220–6225.
7. Lauhon, L. J.; Ho, W. Single-Molecule Chemistry and Vibrational Spectroscopy: Pyridine and Benzene on Cu(001). *J. Phys. Chem. A* **2000**, *104*, 2463–2467.
8. Lee, J.-G.; Ahner, J.; Yates, J. T., Jr. Adsorption Conformation of Chemisorbed Pyridine on the Cu(110) Surface. *J. Chem. Phys.* **2001**, *114*, 1414–1419.
9. Lee, J.-G.; Ahner, J.; Yates, J. T., Jr. Adsorption Geometry of 4-Picoline Chemisorbed on the Cu(110) Surface: A Study of Forces Controlling Molecular Self-Assembly. *J. Am. Chem. Soc.* **2002**, *124*, 2772–2780.
10. Dougherty, D. B.; Lee, J.; Yates, J. T., Jr. Role of Conformation in the Electronic Properties of Chemisorbed Pyridine on Cu(110): An STM/STS Study. *J. Phys. Chem. B* **2006**, *110*, 11991–11996.
11. Hou, J. Q.; Kang, H. S.; Kim, K. W.; Hahn, J. R. Binding Characteristics of Pyridine on Ag(110). *J. Chem. Phys.* **2008**, *128*, 134707.
12. Atodiresei, N.; Caciuc, V.; Franke, J.-H.; Blügel, S. Role of the van der Waals Interactions on the Bonding Mechanism of Pyridine on Cu(110) and Ag(110) Surface: First-Principles Study. *Phys. Rev. B* **2008**, *78*, 045411.
13. Ning, Z.; Polanyi, J. C. Surface Aligned Reaction. *J. Chem. Phys.* **2012**, *137*, 091706.
14. Ning, Z.; Polanyi, J. C. Charge Delocalization Induces Reaction in Molecular Chains at a Surface. *Angew. Chem., Int. Ed.* **2013**, *52*, 320–324.
15. Ning, Z.; Polanyi, J. C. Catalyzed Surface-Aligned Reaction, H(ad)+H_2(ad)=H_2(g)+H(ad) on Coinage Metals. *Z. Phys. Chem.* **2013**, *227*, 1501–1510.
16. Dougherty, D. B.; Lee, J.; Yates, J. T., Jr. Assembly of Linear Clusters of Iodobenzene Dimers on Cu(110). *J. Phys. Chem. B* **2006**, *110*, 20077–20080.
17. Komeda, T.; Kim, Y.; Fujita, Y.; Sainoo, Y.; Kawai, M. Local Chemical Reaction of Benzene on Cu(10) *via* STM-Induced Excitation. *J. Chem. Phys.* **2004**, *120*, 5347–5352.
18. Lesnard, H.; Lorente, N.; Bocquet, M.-L. Theoretical Study of Benzene and Pyridine STM-Induced Reactions on Copper Surfaces. *J. Phys.: Condens. Matter* **2008**, *20*, 224012.
19. Bushell, J.; Carley, A. F.; Coughlin, M.; Davies, P. R.; Edwards, D.; Morgan, D. J.; Parsons, M. The Reactive Chemisorption of Alkyl Iodides at Cu(110) and Ag(111) Surfaces: A Combined STM and XPS Study. *J. Phys. Chem. B* **2005**, *109*, 9556–9566.
20. Horcas, I.; Fernandez, R.; Gomez-Rodriguez, J. M.; Colchero, J.; Gomez-Herrero, J.; Baro, A. M. WSXM: A Software for Scanning Probe Microscopy and a Tool for Nanotechnology. *Rev. Sci. Instrum.* **2007**, *78*, 013705.
21. Perdew, J. P.; Burke, K.; Ernzerhof, M. Generalized Gradient Approximation Made Simple. *Phys. Rev. Lett.* **1996**, *77*, 3865–3868.
22. Blöchl, P. E. Projector Augmented-Wave Method. *Phys. Rev. B* **1994**, *50*, 17953–17979.
23. Kresse, G.; Joubert, D. From Ultrasoft Pseudopotentials to the Projector Augmented-Wave Method. *Phys. Rev. B* **1999**, *59*, 1758–1775.
24. Kresse, G.; Furthmüller, J. Efficiency of *Ab-Initio* Total Energy Calculations for Metals and Semiconductors Using a Plane-Wave Basis Set. *Comput. Mater. Sci.* **1996**, *6*, 15–50.
25. Kresse, G.; Furthmüller, J. Efficient Iterative Schemes for *Ab Initio* Total-Energy Calculations Using a Plane-Wave Basis Set. *Phys. Rev. B* **1996**, *54*, 11169–11186.
26. Hammer, B.; Hansen, L. B.; Nørskov, J. K. Improved Adsorption Energetics within Density-Functional Theory Using Revised Perdew−Burke−Ernzerhof Functionals. *Phys. Rev. B* **1999**, *59*, 7413–7421.
27. Grimme, S. Semiempirical GGA-Type Density Functional Constructed with a Long-Range Dispersion Correction. *J. Comput. Chem.* **2006**, *27*, 1787–1799.
28. Köhler, L.; Kresse, G. Density Functional Study of CO on Rh(111). *Phys. Rev. B* **2004**, *70*, 165405.
29. Ji, W.; Lu, Z.-Y.; Gao, H. Electron Core−Hole Interaction and Its Induced Ionic Structural Relaxation in Molecular Systems under X-ray Irradiation. *Phys. Rev. Lett.* **2006**, *97*, 246101.